MICROCOPY RESOLUTION TEST CHART

NATIONAL BUREAU OF STANDARDS-1963-A

AFWAL-TR-84-4083

CHARACTERIZATION OF THERMALLY TREATED
GALLIUM ARSENIDE BY LASER-RAMAN AND
AUGER SPECTROSCOPY

Neil T. McDevitt
William L. Baun
Mechanics and Surface Interactions Branch
Nonmetallic Materials Division

James S. Solomon
University of Dayton Research Institute
Dayton, Ohio 45469

October 1984

Final Report for Period March 1983 to December 1983

MATERIALS LABORATORY
AIR FORCE WRIGHT AERONAUTICAL LABORATORIES
AERONAUTICAL SYSTEMS DIVISION
WRIGHT-PATTERSON AIR FORCE BASE, OHIO 45433
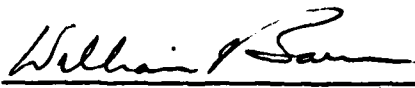
DTIC
ELECTE
DEC 11 1984

B

84   12   08   031

NEIL T. McDEVITT, Project Engineer　　　　WILLIAM L. BAUN, Project Engineer
Surface/Phenomena/Interactions　　　　　　Surface/Phenomena/Interactions

FOR THE COMMANDER

STEPHEN W. TSAI
Chief, Mechanics & Surface Interactions Branch
Nonmetallic Materials Division

REPORT DOCUMENTATION PAGE

1a. REPORT SECURITY CLASSIFICATION Unclassified		1b. RESTRICTIVE MARKINGS		
2a. SECURITY CLASSIFICATION AUTHORITY		3. DISTRIBUTION/AVAILABILITY OF REPORT Approved for public release; distribution unlimited.		
2b. DECLASSIFICATION/DOWNGRADING SCHEDULE				
4. PERFORMING ORGANIZATION REPORT NUMBER(S) AFWAL-TR-84-4083		5. MONITORING ORGANIZATION REPORT NUMBER(S)		
6a. NAME OF PERFORMING ORGANIZATION Materials Laboratory	6b. OFFICE SYMBOL (If applicable) MLBM	7a. NAME OF MONITORING ORGANIZATION		
6c. ADDRESS (City, State and ZIP Code) Air Force Systems Command Wright-Patterson Air Force Base, OH 45433		7b. ADDRESS (City, State and ZIP Code)		
8a. NAME OF FUNDING/SPONSORING ORGANIZATION	8b. OFFICE SYMBOL (If applicable)	9. PROCUREMENT INSTRUMENT IDENTIFICATION NUMBER		
8c. ADDRESS (City, State and ZIP Code)		10. SOURCE OF FUNDING NOS.		

		PROGRAM ELEMENT NO.	PROJECT NO.	TASK NO.	WORK UNIT NO.
11. TITLE (Include Security Classification)			2423	24230153	#50

12. PERSONAL AUTHOR(S)
Neil T. McDevitt, William L. Baun, and James Solomon

13a. TYPE OF REPORT In-house	13b. TIME COVERED FROM 3/83 TO 12/83	14. DATE OF REPORT (Yr., Mo., Day) October 1984	15. PAGE COUNT 42

16. SUPPLEMENTARY NOTATION

17. COSATI CODES			18. SUBJECT TERMS (Continue on reverse if necessary and identify by block number)
FIELD	GROUP	SUB. GR.	gallium arsenide, Raman spectroscopy, oxide films

19. ABSTRACT (Continue on reverse if necessary and identify by block number)

Thermally treated (100) GaAs crystals were characterized by Raman and Auger spectroscopy. Studies were carried out at intervals between $200°C$ and $750°C$. It was difficult to detect any oxide films at temperatures below $450°C$ by Raman spectroscopy. Films grown at $450°C$ were homogeneous and $240Å$ thick. Both Raman and Auger spectroscopy indicate the films consist of Ga_2O_3 and crystalline arsenic dispersed throughout the film. A white dense film was grown at $750°C$ and Raman data indicated it was primarily βGa_2O_3.

gallium oxide

beta gallium oxide.

20. DISTRIBUTION/AVAILABILITY OF ABSTRACT UNCLASSIFIED/UNLIMITED ☒ SAME AS RPT. ☐ DTIC USERS ☐	21. ABSTRACT SECURITY CLASSIFICATION Unclassified	
22a. NAME OF RESPONSIBLE INDIVIDUAL N. T. McDevitt	22b. TELEPHONE NUMBER (Include Area Code) 513-255-5892	22c. OFFICE SYMBOL AFWAL/MLBM

DD FORM 1473, 83 APR   EDITION OF 1 JAN 73 IS OBSOLETE.

FOREWORD

This technical report was prepared by N. T. McDevitt and
W. L. Baun of the Mechanics and Surface Interactions Branch,
Nonmetallic Materials Division, Materials Laboratory, Air Force
Wright Aeronautical Laboratories, and J. S. Solomon, University
of Dayton Research Institute. The work was initiated under
Project 2423 and WUD #50, "Surface and Interface Properties,"
monitored by Dr. T. W. Haas.

This report covers work performed in-house during the period
March 1983 to December 1983.

The authors are grateful to Mr. Don Thomas for his technical
assistance with the Auger data.

DTIC
ELECTE
DEC 1 1 1984
S D
B

Accession For	
NTIS GRA&I	✔
DTIC TAB	☐
Unannounced	☐
Justification	
By	
Distribution/	
Availability Codes	
Dist	Avail and/or Special
A-1	

TABLE OF CONTENTS

LIST OF ILLUSTRATIONS

LIST OF TABLES

SECTION I
INTRODUCTION

Gallium arsenide as a semiconductor has a considerable technological involvement in areas relating to the manufacture and development of electronic devices and their associated systems. In order to realize the full potential of this material in sophisticated electronic systems we need a more definitive understanding of the chemistry of the surface. The factors influencing the chemical and physical properties of the surface are many; however, one of the more important studies in the research of this material is the effect of thermal treatment. A gallium arsenide wafer may be subjected to a thermal anneal at various times during the processing of a device. By heating a GaAs wafer various chemical properties of the surface can be obtained through outdiffusion of impurities contained in the bulk, and by changing the stoichiometry of the bulk crystal.

The need to understand the chemistry of semiconductor surfaces has led to a great many studies utilizing a variety of analytical instruments. One of these systems, Raman spectroscopy, has been shown to provide useful information on characteristic properties of compound semiconductors (References 1-4). Due to the large refractive index of GaAs at 4880Å, laser-Raman spectroscopy can give information about the near surface. The main emphasis of this report will be on the information obtained by laser-Raman and Auger spectroscopy from thermally treated gallium arsenide crystals.

SECTION II
INELASTIC LIGHT SCATTERING SELECTION
RULES FOR A GaAs CRYSTAL

When electromagnetic radiation interacts with a crystal
lattice a photon may be absorbed provided the wave vector and
the energy are conserved. The wave vector is extremely small
compared with the wave vector corresponding to the edge of the
Brillouin zone. Since the wave vector of light is much smaller
than the Brillouin-zone boundary wave vector, first-order inelastic
light scattering will allow us to study the excitations near the
center of the Brillouin zone where the wave vector is essentially
zero ($K \approx 0$). This first order Raman scattering allows us to
observe the vibrations of a crystal called lattice modes. Lattice
modes are the motions of the groups, within a crystal, relative
to one another. Lattice modes give rise to Raman scattering when
a change in one or more components of the polarizability of the
crystal occurs during a vibration. The Raman tensor that
describes this physical parameter for each mode is governed by
the symmetry of the scattering crystal.

We can use the correlation method (Reference 5) to derive
the vibrational selection rules for the crystals of interest in
this study. The crystal structure of the material dictates the
orientation of all groups within the crystal. The crystal lattice
will determine the space group, which will contain the site
symmetries of the atoms in the unit cell. The crystallographic
unit cell may be identical with the Bravais cell or it may be
larger by some simple multiple. The Bravais space cell is used
by molecular spectroscopists to obtain the irreducible repre-
sentation for the lattice vibrations. The number of molecules
per Bravais unit cell will give us the number of equivalent atoms
of each kind that are present. From the space group and the x-ray
crystallographic tables we may determine the site symmetry of each
atom. The symmetry species are not identified for each equivalent
set of atom displacements in the site. The displacements we
describe will become the lattice vibrations in the crystal. Know-
ing the site species for these displacements, we can relate each

species of the site group to a species of the factor group. This correlation explicitly identifies the species of the lattice vibration in the crystal and further allows prediction of the number of infrared and/or Raman active vibrations.

The gallium arsenide crystal has the structure of the mineral zinc blende. The zinc blende structure is essentially the diamond crystal structure with the exception that it has two elements describing the cell. The atoms of the first element (regardless of whether they are gallium or arsenic) occupy the positions of a face-centered-cubic cell. The atoms of the second element occupy the centers of four small cubes. Both positions are exactly equivalent to each other. The structure of zinc blende and diamond are characterized by identical Bravais lattices (face-centered cubic). However, their space groups of symmetry are different: T_d^2, $F\overline{4}3m$ for zinc blende and O_h^7, $Fd3m$ for diamond.

The conventional unit cube for GaAs is shown in Figure 1. This is the crystallographers unit cell and is four times larger than the Bravais unit cell. Bisection of the cube in Figure 1 generates the (110) plane (Figure 2). GaAs cleaves most readily on this plane. Because of this, almost all of the early experimental work was performed using the (110) surface. GaAs crystals were first grown by the horizontal Bridgeman technique with the most prominent surface being the (111) plane shown in Figure 3. This can be formed by truncation of the unit cell in Figure 1. Most of the GaAs wafers used in present day devices utilize the (100) plane. These crystals are grown using the vertical liquid encapsulated Czochralski technique. The (100) surface may arbitrarily terminate with either Ga or As atoms.

1. FACTOR GROUP ANALYSIS FOR GaAs

The structure of the mineral zinc blende is described in the literature (Reference 6). The space group for this face-centered-cubic (fcc) compound is shown to be T_d^2-$F\overline{4}3m$ with four formula units per cell. However, the molecular spectroscopist may ignore glide planes and screw axis because they will create

3
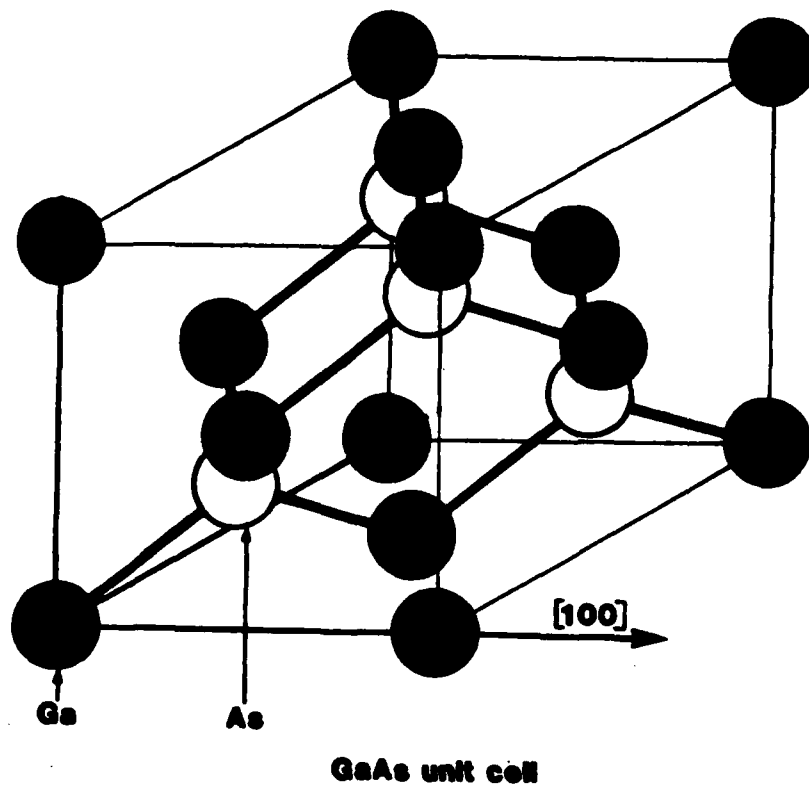
Figure 1. Conventional Unit Cell for GaAs, This Volume Is
Four Times Larger Than the Bravais Cell

Figure 2. Bisection of the GaAs Unit Cell Shows the Make Up of the (110) Plane
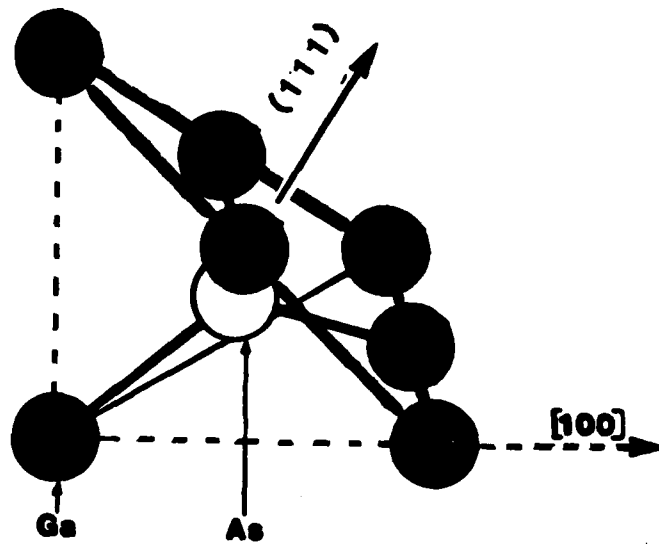
Figure 3. With the Appropriate Truncation of the GaAs Unit
Cell We Can Observe the (111) Plane

redundancies in the calculated optical activity. By constructing a Bravais unit cell that contains only one lattice point, and still displays the full symmetry of the fcc crystal, we can generate a unit cell with just one formula unit instead of four. The site symmetry of each atom may be found in Reference 7. There will be one gallium and one arsenic atom at the site position T_d.

In order to obtain the first-order infrared and Raman activity of the zinc blende crystal requires knowledge of only the properties of the long-wavelength phonon for which the wave vector (K) approximately equals zero. The long-wavelength phonons may then be classified in terms of their symmetry properties by the irreducible representations of the T_d factor group. Utilizing the correlation method, we can find the irreducible representation of each sublattice of the Bravais unit cell is:

$$Ga(T_d) = F_2$$
$$As(T_d) = F_2 \quad .$$

The total activity of the zone-center modes of GaAs are composed of the symmetry GaAs = $2F_2$.

This analysis predicts a total of two normal modes. Of the $2F_2$ modes, one will be associated with the three degrees of translation of the entire unit cell. These are known as the acoustical vibrations and have nearly zero frequency when K=0. These vibrations are of no physical interest in our analysis and may be subtracted from our total activity; therefore,

$$GaAs = 1F_2 \quad .$$

The T_d point-group character table shows the F_2 symmetry species contains both infrared and Raman activity, so the activity predicted for GaAs will appear at the same energies in the infrared and Raman spectrum.

2. FACTOR GROUP ANALYSIS FOR βGa_2O_3

βGa_2O_3 is a compound belonging to the $C_{2h}^3 - C_{2/m}$ space group with two molecules per Bravais unit cell. The site symmetry for the Ga and O atoms is C_s. The irreducible representations for the optically active modes contained in the Bravais unit cell are,

7

$$\beta Ga_2O_3 = 10Ag + 5Bg + 4Au + 8Bu$$

and excluded from this activity are the acoustical modes $1Au+2Bu$. For this compound the Ag and Bg symmetries are Raman active. In the first order spectra all the lattice vibrations that are Raman active are infrared inactive and vice versa.

3. FACTOR GROUP ANALYSIS FOR As_2O_3

The structure of the mineral arsenolite (As_4O_6) is described in the literature (Reference 6). The space group for this face-centered-cubic compound is shown to be O_h^7-Fd3m. There are four molecules per Bravais unit cell. The molecular groups are bound together in close combination to form a molecule with tetrahedral symmetry. These molecules are distributed in the unit cell at the same positions as are the carbon atoms in diamond. Each molecule lies between four others and owing to their tetrahedral shape they pack closely together. The site symmetry for the As atoms is C_{3v}, while the O atoms are on sites having C_{2v} symmetry. The irreducible representations for the optical modes in this crystal are

$$As_2O_3 = 2A_{1g}+2E_g+3F_{1g}+5F_{2g}+2A_{2u}+2E_u+5F_{1u}+3F_{2u}$$

and the irreducible representation for the acoustical mode is found with symmetry F_{1u}. The active optical modes are,

$$As_2O_3 = 2A_{1g}+2E_g+5F_{2g}+4F_{1u}(IR)$$

where the A_{1g}, E_g, and F_{2g} symmetries are Raman active.

4. FACTOR GROUP ANALYSIS FOR As

The structure of the element arsenic is described in Reference 6. The space group for this element is D_{3d}^5=R3m. There are two atoms per Bravais unit cell. The structure is layered and each atom has three closest neighbors and molecules are not formed. The site symmetry for the As atoms is C_{3v}. The irreducible representation for the optical modes in metallic arsenic are:

$$As = 1A_{1g}+1E_g+1A_{2u}+1E_u \quad .$$

8

The irreducible representations for the acoustical modes are $1A_{2u}+1E_u$. Therefore, the first-order vibrations observed will have A_{1g} and E_g symmetry and will be Raman active and infrared inactive. There is no infrared activity for this crystal.

5. FACTOR GROUP ANALYSIS FOR Ga

The space group for gallium is D_{2h}^{18}-Acam. There are four atoms per Bravais cell. The Ga atom has seven neighboring atoms in a layered structure. The layers are composed of slightly irregular flat hexagonal rings of Ga atoms and are similar to the hexagonal nets in the structure of graphite. Since each atom has one nearest neighboring atom, this structure may formally be considered molecular. The site symmetry for the Ga atoms is C_s. The irreducible representation for the optical modes in metallic gallium are

$$Ga = 2A_g+1B_{1g}+1B_{2g}+2B_{3g}+1A_u+2B_{1u}+2B_{2u}+1B_{3u} \quad .$$

The irreducible representations for the acoustical modes are $1B_{1u}+1B_{2u}+1B_{3u}$. The active optical modes are

$$2A_g+1B_{1g}+1B_{2g}+2B_{3g}+1A_u+1B_{1u}+1B_{2u}$$

and the vibrations with symmetry A_g, B_{1g}, B_{2g} and B_{3g} are Raman active and infrared inactive.

SECTION III
THERMAL TREATMENT OF GaAs

In order to realize a MOSFET structure from a single crystal GaAs system a high-quality native oxide must be formed with a minimum of surface state charge. Since a great deal of success has been achieved in forming SiO_2 on silicon with high-temperature processing, it followed that this same procedure should be looked at in processing GaAs. Therefore, the thermally prepared oxide on GaAs has led to a large number of studies (References 8-24). The early studies (References 8-9) indicated that the thermal oxides were not suitable for device applications and the method was not fully investigated. In 1974 (Reference 10) Sealy stated "The thermal oxide growth does not appear to change the near-surface carrier concentration, and the oxide might be a reasonable encapsulant for GaAs." Starting in 1975 a number of workers revived the thermal oxide studies on GaAs. GaAs on being oxidized in oxygen shows no appreciable weight loss below 750°C. Between 750°-850°C a white oxide growth forms and x-ray diffraction studies indicate this product is primarily βGa_2O_3. Thermal oxidation of GaAs in air at lower temperatures, 350°-500°C, show much lower oxidation rates and a two-hour anneal at 450°C will generate a 200Å oxide film.

Investigation of thermally oxidized GaAs crystals with various surface instrumentation has led to inconsistent results. Shiota (Reference 15) measured in-depth profiles of the oxide layer by Auger electron spectroscopy during Ar sputter etching. Their results reveal Ga depletion with an increase in As at the interface. However, Kee (Reference 25) pointed out several errors made by Shiota claiming their results did not take into consideration the change in chemical state of the Ga as the sample was sputtered. Work by other researchers has not led to a good understanding of the compositions of these films or even to a complete agreement between researchers. It is apparent that the understanding of the chemical make-up of thermally treated GaAs crystals remains incomplete and more information on this surface should present some significant information toward a better compositional analysis.

10

SECTION IV
EXPERIMENTAL PROCEDURE

The Raman scattering experiments were performed with
incident laser light of 4880Å. The incoming laser light (200 mW)
was focused on each crystal surface as shown in Figure 4. The
light was polarized perpendicular to the plane of incidence and
the crystal was placed at an angle of 10°-13° from the vertical.
The angle was obtained through the use of a single crystal
goniometer. This setting placed the surface of the crystal at
or below Brewster's angle and allowed for maximum energy transfer
to the crystal. The scattered light was not polarized. The
inelastically backscattered light was collected at 90° from the
incident beam and focused by a lens onto the entrance slit of
a Jarrel Ash double monochromator.

All of the semi-insulating GaAs single crystals used in
this study were obtained commercially. The crystals were cut
from boules grown by the liquid encapsulated Czochralski process.
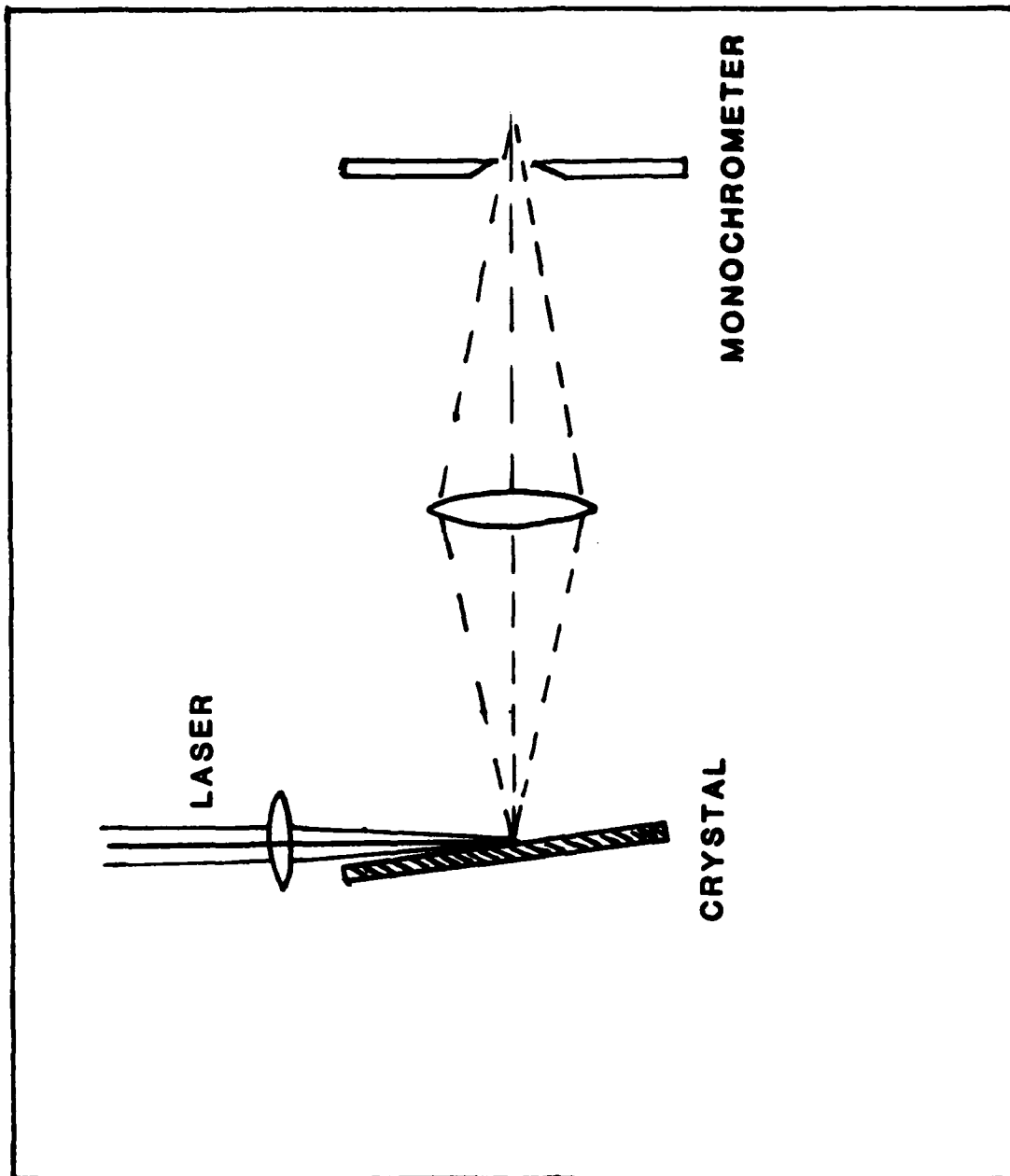The surfaces studied were the (100) plane. No dopants were
added intentionally.

Figure 4. Experimental Set Up for Backscattering Laser of
Single Crystals

SECTION V
EXPERIMENTAL RESULTS

When light is scattered from a solid we are dealing with
a system where all the unit cells are oriented in the same
manner. Therefore, with incident polarized monochromatic light
we can observe scattered light from different axes of the crystal.
Depending on the selection rules for each crystal we may observe
active modes that may be labeled transverse optical phonons (TO),
longitudinal optical phonons (LO), or both. In the case of the
zinc blende structure we can observe the LO, TO, or both modes
depending on the crystal surface being studied. When referenced
to the (100) plane a GaAs crystal should only generate an LO
phonon mode. When reflected from a (110) plane only TO phonons
are allowed and for (111) planes both LO and TO lattice vibra-
tions should be present. Figure 5 shows observed Raman spectra
from the (100) and (111) surfaces of our GaAs wafers. The strong
LO mode (292 cm^{-1}) should be the only observed Raman band from
the (100) surface; however, these crystals were cut slightly off
the (100) plane so a small amount of TO (269 cm^{-1}) mode is observed.
The (111) surface shows a strong TO mode (269 cm^{-1}) and a weaker LO
mode with both modes predicted for this surface. Deviations from
the Raman scattering selection rules can also be observed in GaAs
surfaces that are poorly polished or have surface damage. We
have shown that GaAs belongs to the T_d factor group and a factor
group analysis predicts one Raman active mode: F_2. This triply
degenerate mode contains the 269 cm^{-1}(TO) and the 292 cm^{-1}(LO)
energy bands of GaAs.

A number of researchers (References 26-33) have shown Raman
spectroscopy to be a versatile technique in the study of thin films
on GaAs. The change in the chemical state of the GaAs surface
through thermal treatment is of particular interest to us. We are
reporting on the results obtained in our laboratory and have
placed these data in context with other experimental work.

Most of the samples in this report were heated in air.
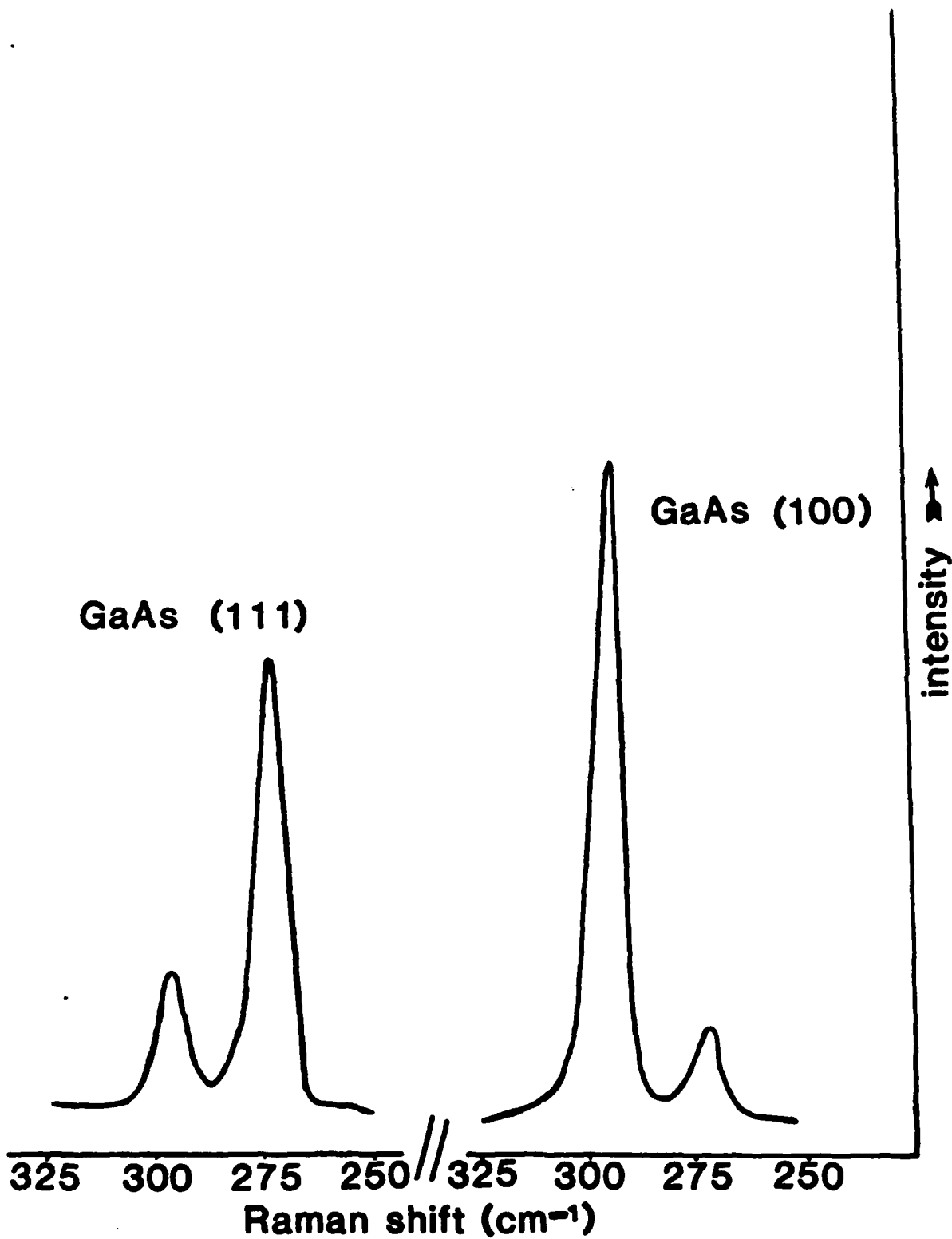Raman reference spectra were obtained on several materials that

Figure 5.   Raman Scattering Spectra from the (111) and (100)
Planes of Single Crystal GaAs

have a high probability of forming on the surface of GaAs when it is heated in air. These materials were obtained as finely divided powders and then pressed into dense pellets for Raman scattering studies. The Raman spectra of the first compound, βGa_2O_3, is shown in Figure 6. Factor group analysis predicts $10A_g$ and $5B_g$ modes. We observe only ten bands in our recorded data. βGa_2O_3 is a weak scatterer and the bands not observed may be due to the poor scattering properties of the powdered sample. The only reasonably strong band was observed at 202 cm^{-1}.

The cubic form of arsenious oxide may also form on heated GaAs although it may not remain on the surface for long since it sublimes at 200°C. The reference spectra of As_2O_3 is shown in Figure 7. Factor group analysis predicts nine active Raman modes. We observe only seven from the powder sample. Unlike βGa_2O_3, cubic As_2O_3 is a very strong scatterer and should not be difficult to detect if it is present on the GaAs surface.

1.   OXIDATION STUDIES

Thermal oxidation of one centimeter square wafers of GaAs was carried out in a simple tube furnace with a normal flow of air. Samples were submitted to temperatures between 200° and 750°C for one hour. There were no apparent visible changes in the samples heated at 350°C and below. The Raman spectra of these samples were identical to room temperature GaAs exhibiting the LO and TO modes at 292 and 269 cm^{-1} (Figure 8a). Samples heated to 450°C for one hour appeared gold in color. The Raman spectra (Figure 8b) shows two new bands at 200 and 259 cm^{-1} that completely overshadow the phonon modes of the GaAs crystal.

Ellipsometric measurements made on this sample indicate a film thickness of 240Å. Samples heated to 550°C were blue in appearance. Data obtained by Raman scattering for this sample is shown in Figure 9a. The new bands observed in Figure 8b have decreased in intensity for this sample and the LO and TO modes of GaAs are more prominent. Film growth did not appear to be homogeneous on the 550°C sample and ellipsometric measurements were inconclusive as to film thickness. At 650°C the sample was

15
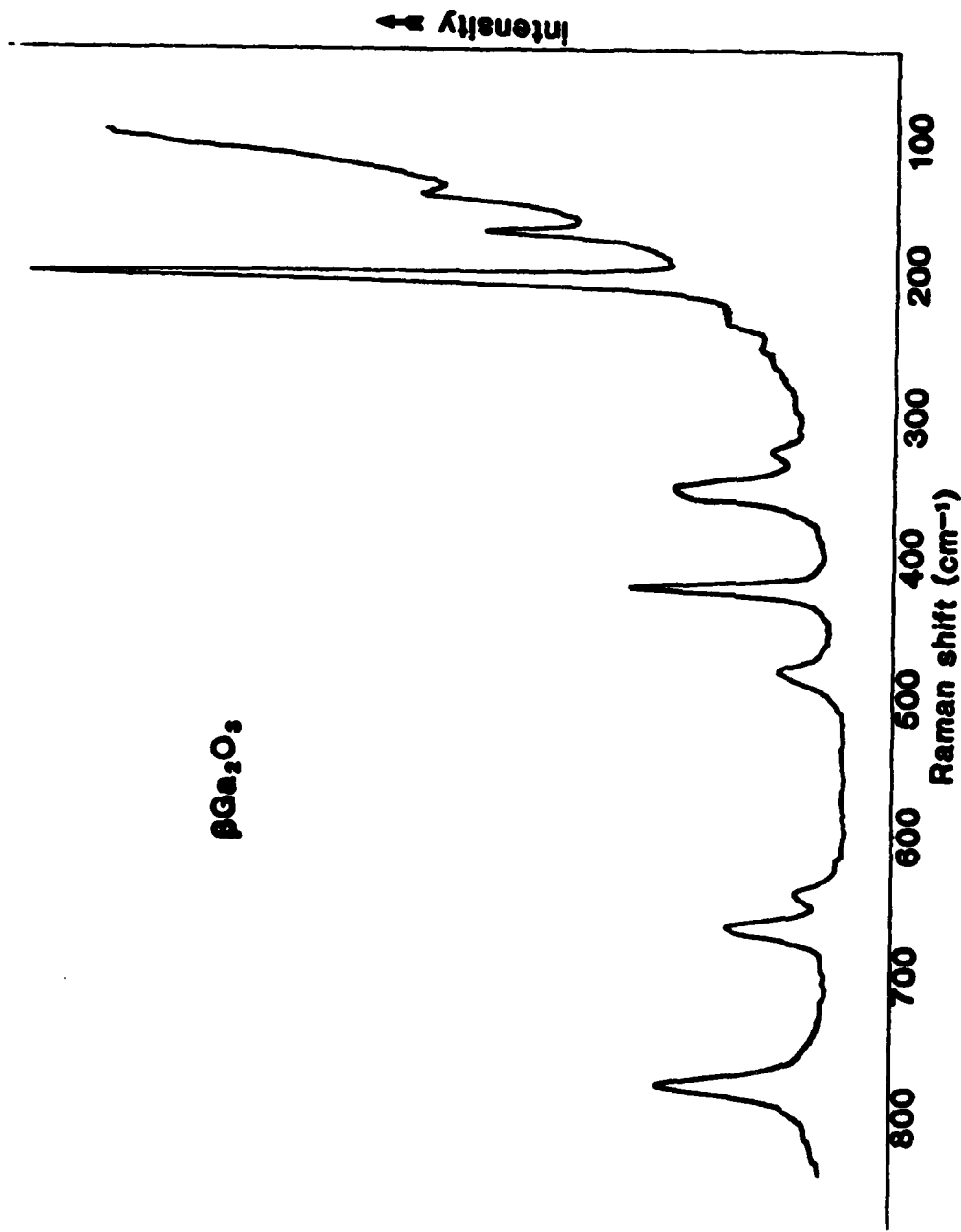
Figure 6. Raman Spectrum of Powdered Reference Material βGa_2O_3
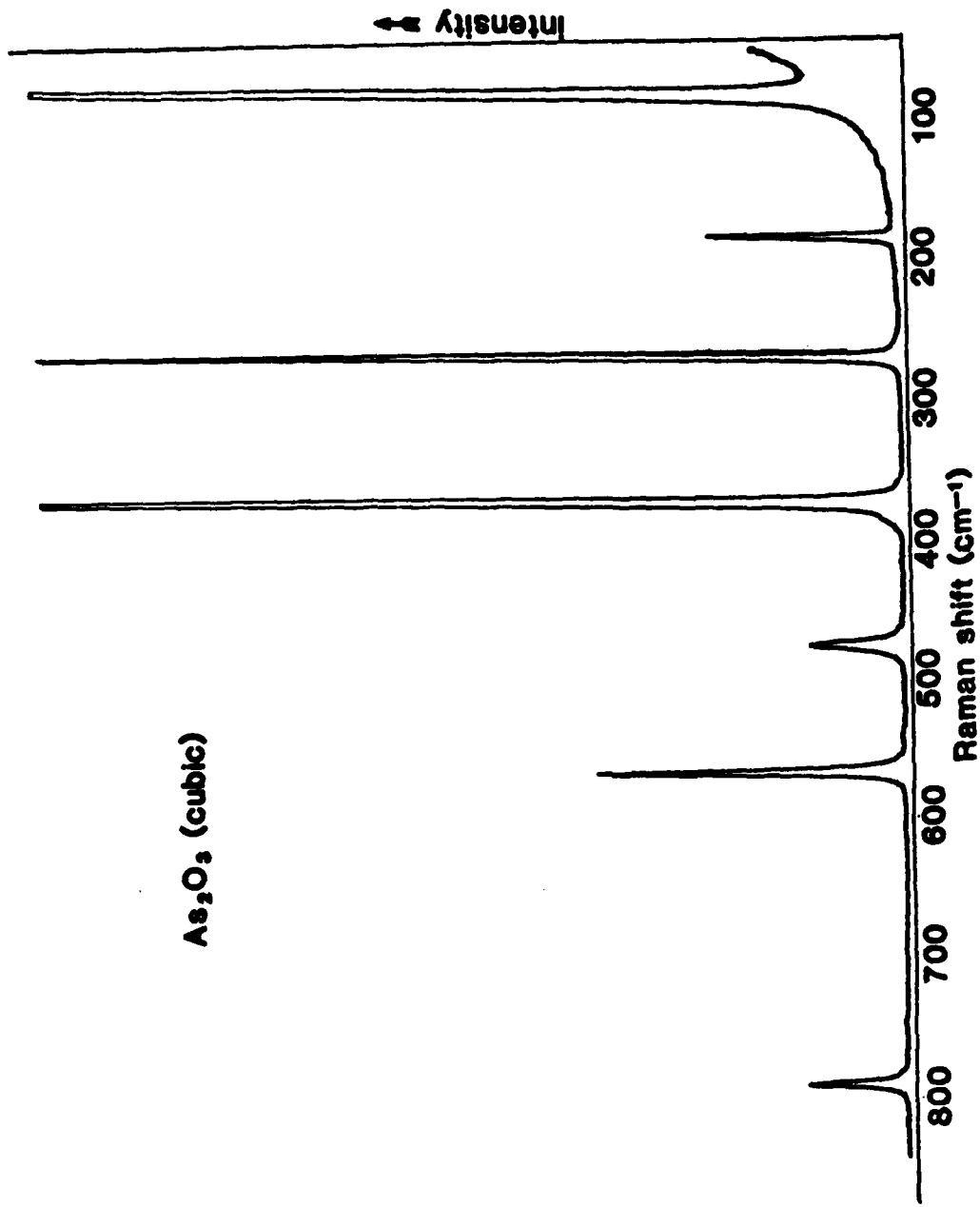
Figure 7. Raman Spectrum of Powdered Reference Material As$_2$O$_3$ (Cubic)

17

a

350°C 60 min

LO —— As

TO

TO

GaAs

LO

b

450°C 60min

intensity ➤

500   400   300   200   100
Raman shift (cm⁻¹)

Figure 8.   Raman Spectra of Thermally Treated GaAs Crystals
            at 350°C (a), and 450°C (b)

Figure 9.   Raman Spectra of Thermally Treated GaAs Crystals
at 550°C (a), and 650°C (b)

19

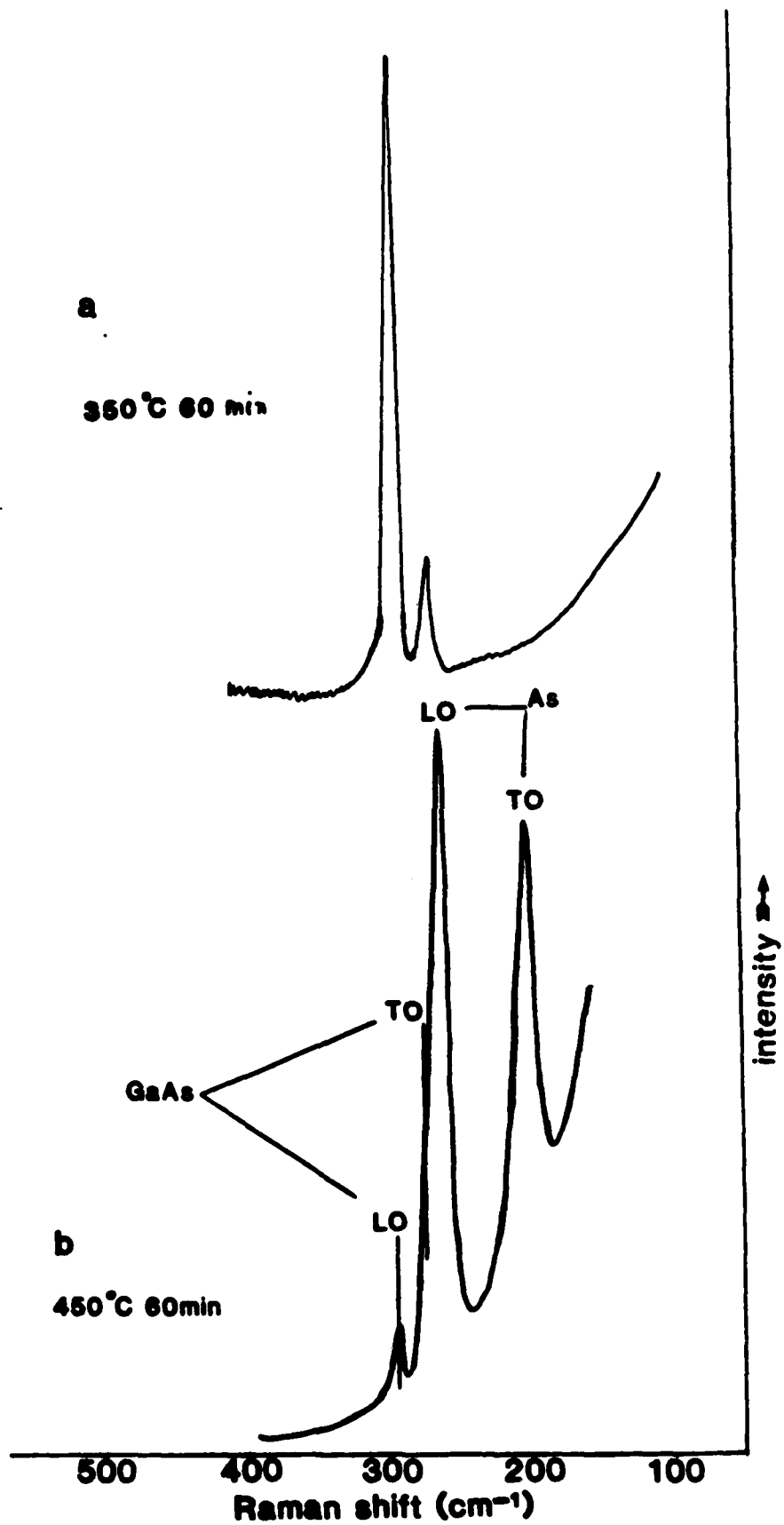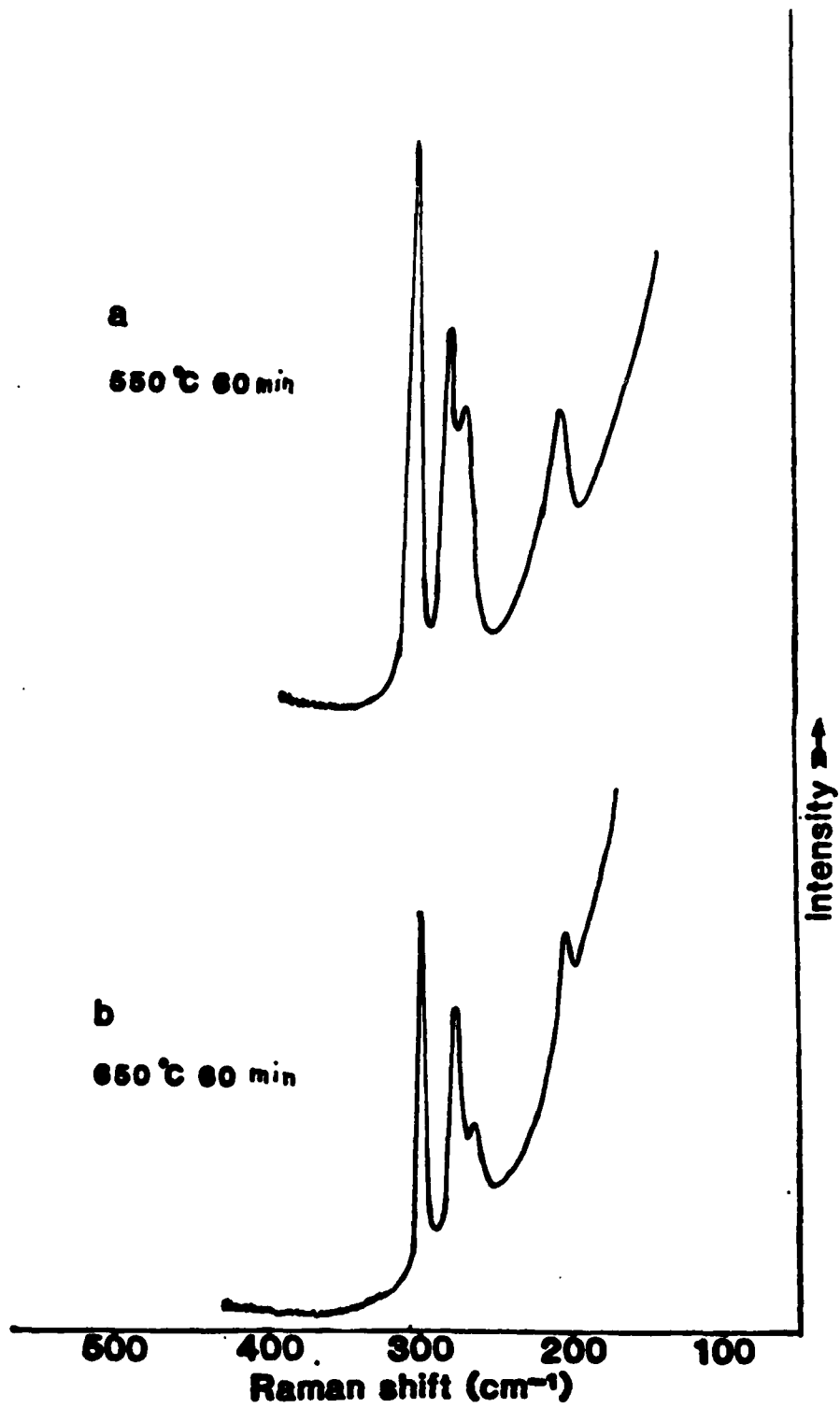a bluish color and the spectrum (Figure 9b) was less intense than the previous sample with the 200 and 259 cm^{-1} bands becoming very weak in intensity.

Figure 10 shows the Raman spectrum of a sample heated to 750°C for 30 minutes. A white dense film covered the surface of this wafer. With the exception of two bands these results match the Raman data obtained from the βGa_2O_3 oxide reference spectrum. Table 1 compares the frequencies of the two reference compounds and the thermally oxidized sample. An identical wafer of GaAs was heated to 750°C for 30 minutes with an argon environment. No film was apparent on this sample and the Raman spectrum showed only the LO and TO modes of GaAs. There was no indication of bands at 200 and 259 cm^{-1}.

The 450°C, 60-minute sample was treated with a 1:1 solution of warm (40°C) $HCl:H_2O$. Figure 11b shows the results of an eight minute wash in this solution. The 200 and 259 cm^{-1} bands have decreased in intensity. Figure 11c shows the low frequency bands are no longer observable after a 16-minute wash in the HCl solution.

Concentrated nitric acid will etch GaAs surfaces and selectively precipitate As_2O_3 (cubic)(Reference 34). For our study this is an interesting reaction and allowed us to observe a film of As_2O_3 directly on GaAs by Raman scattering. Figure 12 (upper curve) shows two strong Raman bands from a film generated by a HNO_3 etch. These two bands match the 268 and 370 cm^{-1} bands observed from the cubic As_2O_3 reference spectrum. This sample was then annealed at 450°C for 60 minutes in air, and the Raman spectrum is shown in the lower curve. The strong bands seen in the upper curve are no longer observable.
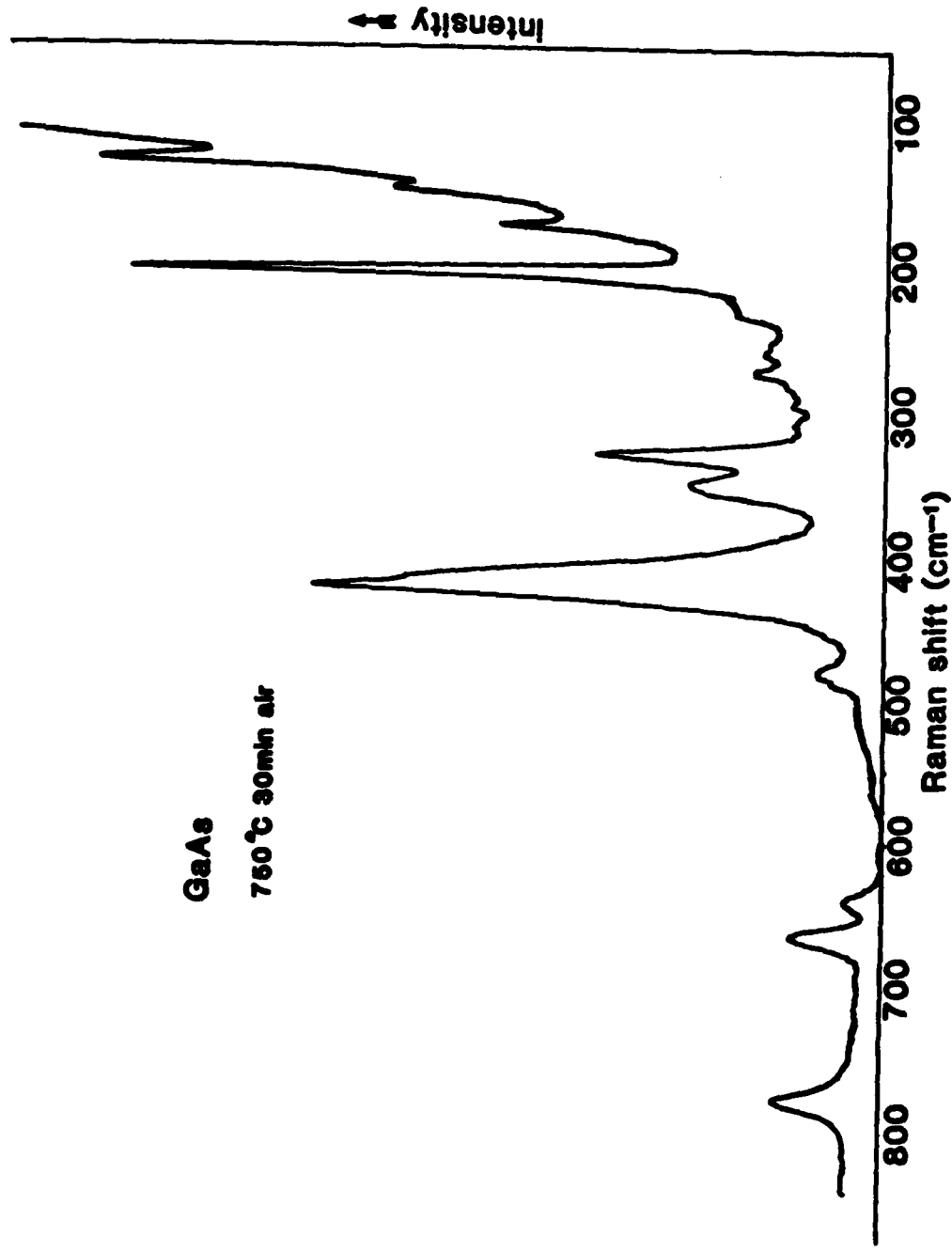
Figure 10. Raman Scattering from a Film Generated on Single Crystal GaAs at a Temperature of 750°C

21

TABLE 1

LATTICE FREQUENCIES IN CM^{-1} FOR βGa_2O_3, As_2O_3 AND THERMALLY OXIDIZED GaAs

βGa_2O_3	Oxidized GaAs	As_2O_3 (cubic
		87
	126	
140	140	
168	168	
		184
202	202	
	270	268
328	334	
354	354	
		370
	420	
426	426	
		470
486	486	
		560
649	649	
671	671	
		780
788	788	

22

Figure 11.   Raman Spectra Obtained from a Film on GaAs Generated
              at 450°C Then Etched for 8 and 16 Minutes in a 1:1
              Solution of HCl: H_2O

23

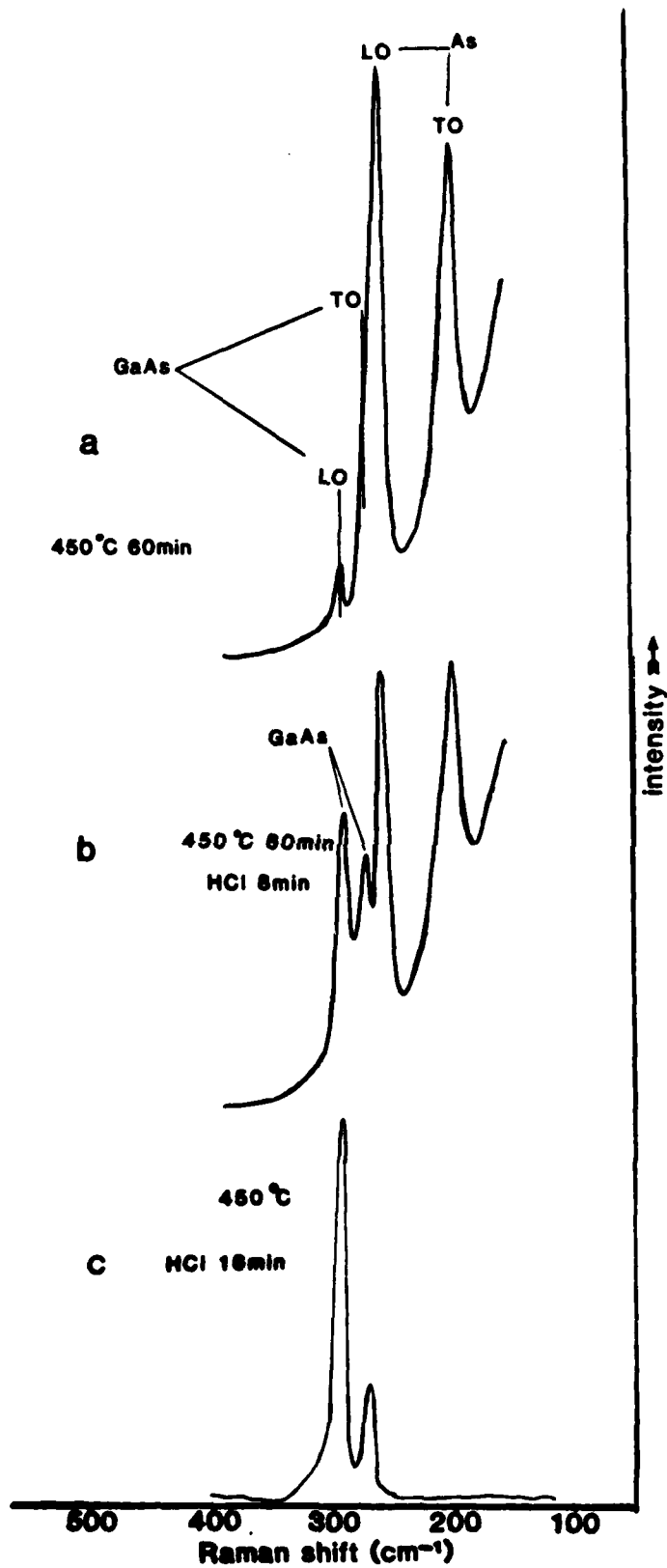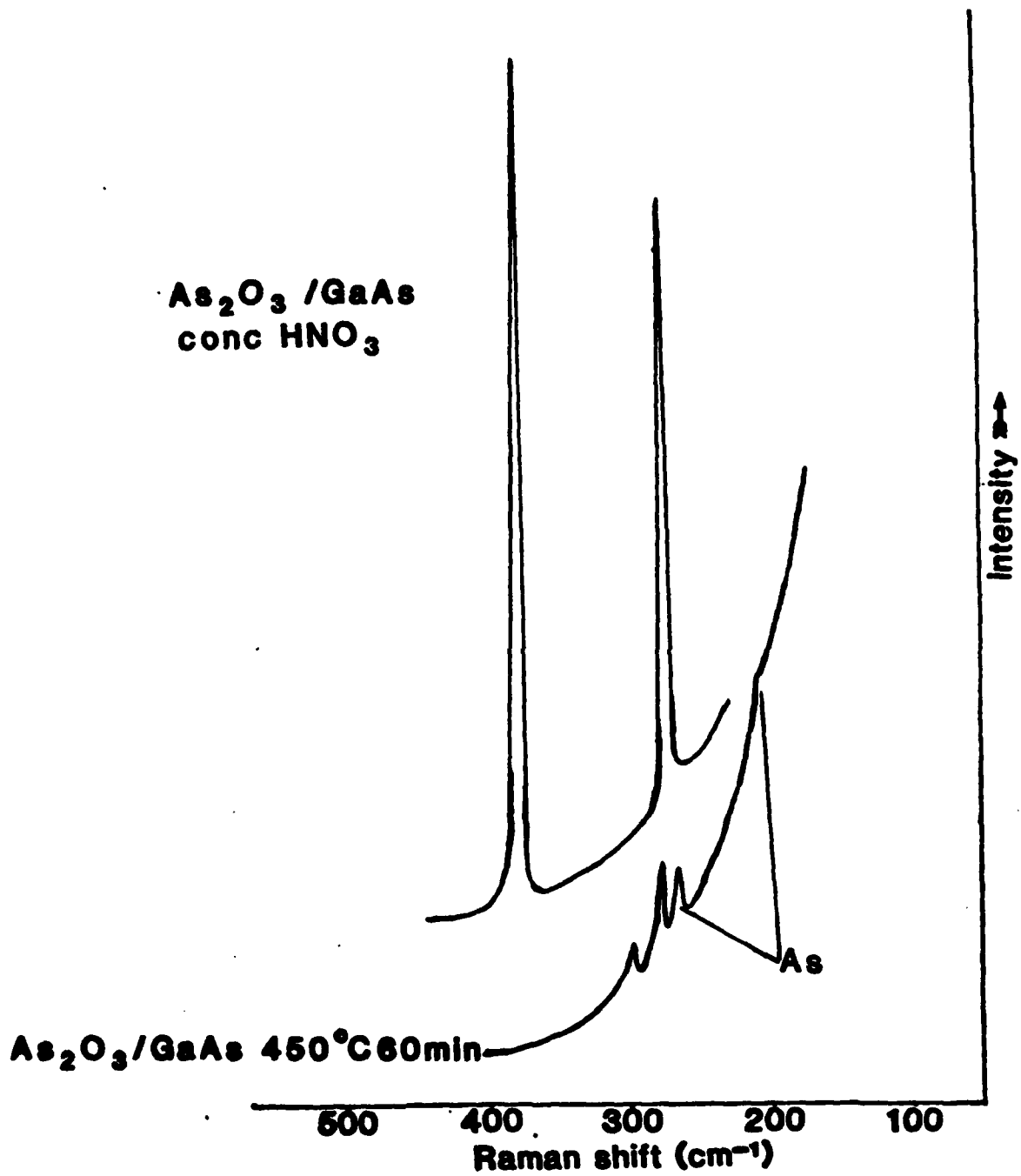Figure 12. Raman Spectra Obtained from a Film on GaAs Generated by a 20 Second Dip in Concentrated HNO_3 Acid Then Annealed at 450°C for 60 Minutes

24

2.   AUGER DEPTH PROFILE ANALYSIS

A number of literature studies have indicated the excess As appears at the interface between the oxides and the substrate GaAs (References 28,36). Since the Raman data (Figure 11) could be misleading as to a discreet arsenic layer we submitted these same samples, Figure 8b thermally treated and Figure 12 chemically etched, to an Auger depth profile.

Figure 13A shows the Auger depth profiles of O, Ga, and As obtained by sputtering the surface with a 2 kV argon ion beam at a current density of 1.6×10^{-5} A/cm^2. The Auger analysis was performed using a 3 kV primary electron beam with a current density of 0.2 A/cm^2. These profiles were constructed by using the O KLL, Ga, and As $L_3 M_{4,5} M_{4,5}$ d(E·N)/dE peak-to-peak heights. Each energy curve was multiplied by a factor in order to normalize all profiles to a 10 volt signal level. The As and O profiles cross each other after approximately four minutes of sputtering. This corresponds to an approximate depth of 180Å. Ga and O decrease in signal as the layer is sputtered indicating these elements are the only ones on the surface in a reasonable concentration. After sputtering for five minutes the Ga signal begins to increase and together with As reaches the level for bulk GaAs after seven minutes. The dip in the Ga profile has been attributed to a depletion of this element at the interface. If this same data is taken as a ratio (As/Ga) with As we naturally have an artificial increase of As at the interface. In reality the dip is an artifact created by the changing peak shape of the Ga $L_3 M_{4,5} M_{4,5}$ signal on going from Ga_2O_3 to GaAs. This effect can be eliminated (Reference 38), as shown in Figure 13B, if the area under the E·N peaks is used to construct the profile. Figure 14 shows the structure of the Ga and As d(E·N)/dE peaks after various sputtering times. There is a definite change in the spectral configuration of the Ga signal from 0 to 9 minutes, while the configuration of the 2 and 9 minute signals from As remains unchanged. The Ga data can be explained as signals arising from Ga associated with oxygen (0 minutes) to Ga associated with As (9 minutes), and this can be seen from Figure 15 where the Ga signal from the reference material Ga_2O_3

25
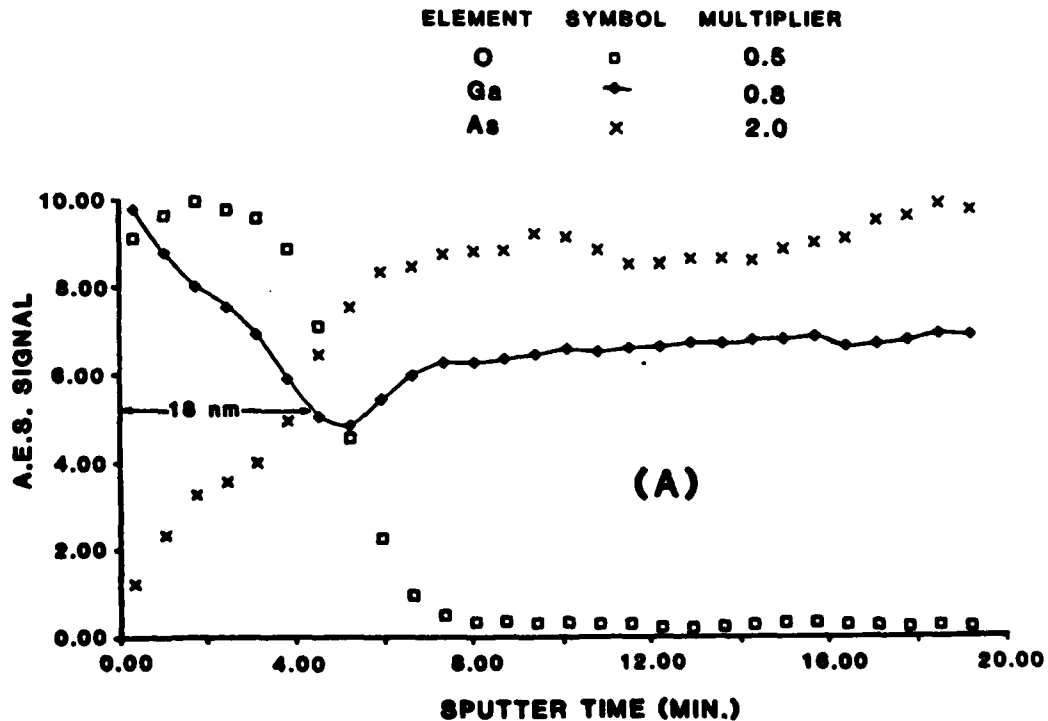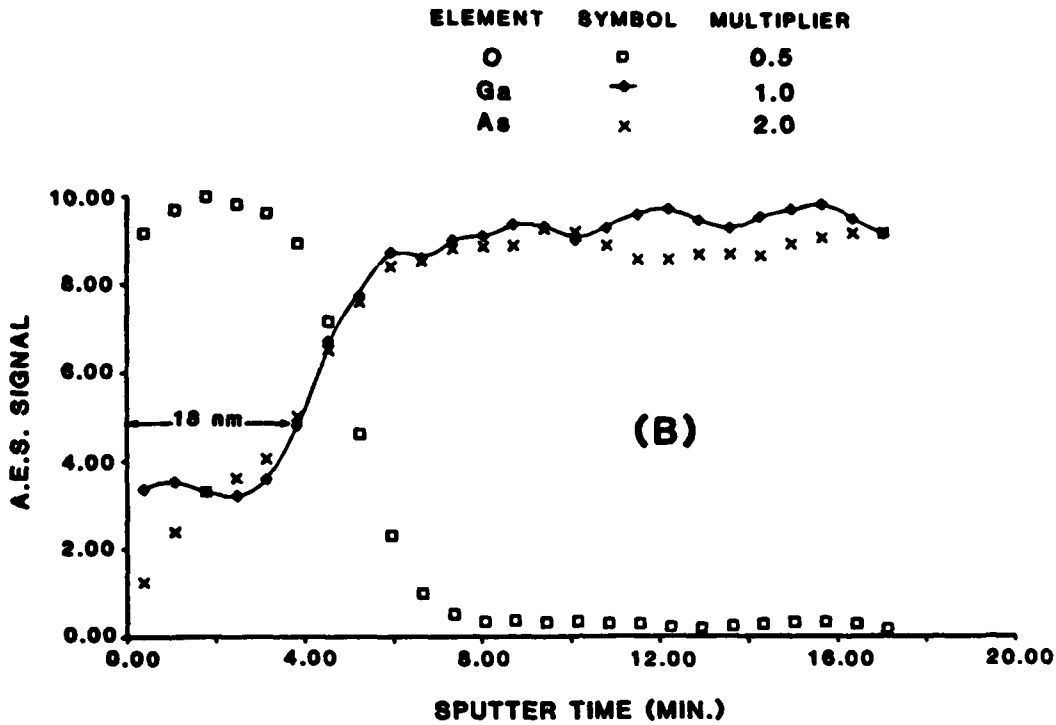
Figure 13. Auger Sputter Profiles of O, Ga, and As from Thermally Oxidized (450°C, 60 min.) GaAs Constructed from d(E·N)/dE Peak-to-Peak Height (A) and (B) Same as A Except Ga Profile Constructed from Area Under E·N Peak

26
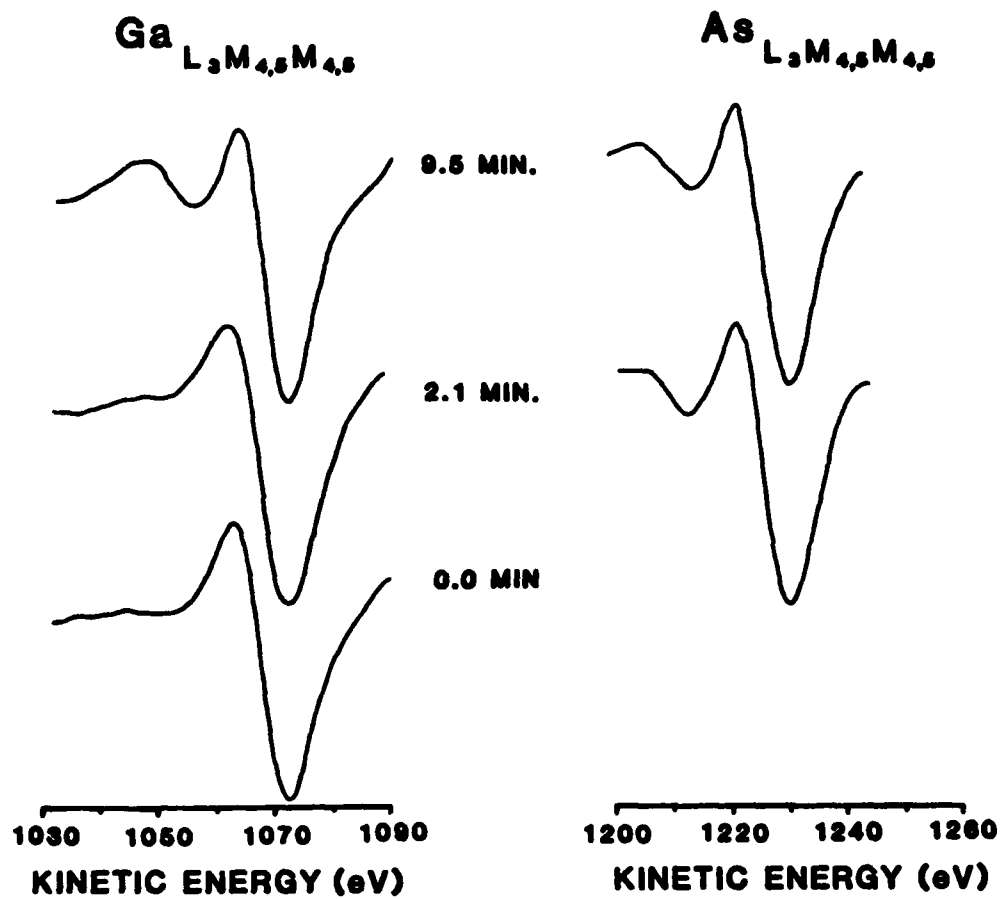
Figure 14. Sputter Profiles for Thermally Oxidized GaAs
(450°C, 60 min.) by Recording the d(E·N)/dE
Peaks of Ga and As $L_3M_{4,5}M_{4,5}$
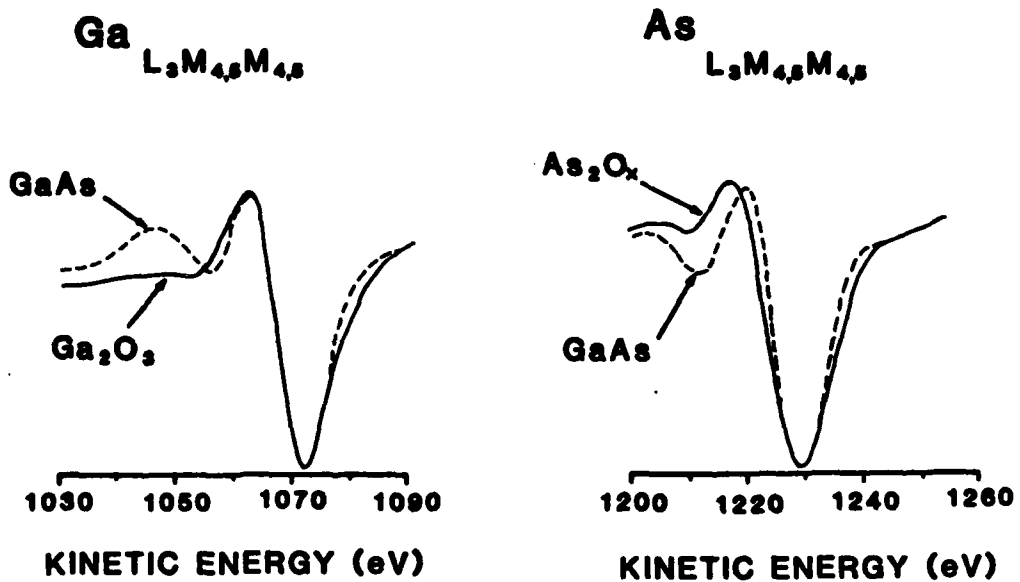
Figure 15. Profiles from Sputter Cleaned GaAs, Ga_2O_3 and a Film of As_2O_3 on GaAs

and GaAs are recorded. Figure 15 also shows a spectral change in the As peak when recorded from GaAs and As_2O_3 on GaAs. The As peak from As_2O_3 is reported as As_2O_x since we are unsure of the effect of the electron beam on this compound.

SECTION VI
DISCUSSION

The examination of the Raman spectra of GaAs single crystals by means of laser excitation is a potentially powerful technique for studying the near surface chemistry of this material. Raman active vibrations for these single crystals can be deduced from the symmetry of the unit cell. Distortions of this symmetry can be observed through the lattice vibrations of the crystal.

First order Raman scattering was observed from the (100) plane of GaAs at 269 and 292 cm^{-1}. The active LO phonon at 292 cm^{-1} is prominent in this orientation. The TO phonon should be inactive from the (100) plane; however, it does appear as a weak band at 269 cm^{-1}. The intensities of these two bands are reversed in the (111) plane scattering. The intensity of the 269 cm^{-1} band from the (100) plane can vary with surface characteristics generated by mechanical or chemical treatments.

From the data shown in Table 1 it is clear that the film grown on GaAs at 750°C, for 60 minutes in air, is primarily βGa_2O_3. The data points that do not match up with the reference spectrum occur at 270, 334, and 420 cm^{-1}. The 270 cm^{-1} band is weak in intensity but could indicate the presence of a small amount of As_2O_3; however, we would also expect the appearance of a band at 370 cm^{-1} because it is the most intense band in As_2O_3 and this band is not observed. The two bands at 334 and 420 cm^{-1} probably indicate the presence of another crystal form of Ga_2O_3.

The thermal oxidation of GaAs has been reviewed by Schwartz (Reference 11) and the data reported here agrees quite well with the literature. The oxidation rate of GaAs below 700°C is very slow. The first noticeable growth is at 450°C. Figure 8b shows the Raman spectrum exhibited by the film grown at 450°C. The two bands observed at 200 and 259 cm^{-1} were first reported by Cape (Reference 35). He was not able to give a specific assignment to these bands and left them unexplained. Farrow (Reference 36) in his work pointed to the Raman work on crystalline As by Zittner (Reference 37) and concluded the 200 and 259 cm^{-1} bands were due to excess As at the GaAs/oxide interface.

The factor group analysis of crystalline As predicts two active Raman modes and are assigned to the symmetry A_{1g} and E_g. The A_{1g} mode represents the motion of the LO lattice vibrations and the E_g mode represents the TO vibrations. The 200 cm^{-1} band is assigned to the TO mode and the 259 cm^{-1} band to the LO mode (Figure 8). The total film thickness for this sample has been determined to be 240Å. The intensity of the crystalline As bands can be attributable to the large complex refractive index of this material. Ga_2O_3 is the major component of this film; however, since it is a poor Raman scatterer it cannot be observed. Figures 9a and 9b show an apparent decrease in the intensity of the arsenic TO and LO modes on going to higher anneal temperatures. The decrease in intensity of these bands is not caused by less arsenic in the film (crystalline As does not sublime until 615°C) but to the increase of Ga_2O_3 component of the film. The concentration of Ga_2O_3 is still not large enough to observe Raman scatter from this component. The low refractive index of Ga_2O_3 does, however, allow laser excitation to again see the bulk GaAs and make the 269 and 292 cm^{-1} lattice modes observable.

The etch study with HCl (Figure 11) did not indicate any abrupt transitions in the intensity of Raman bands due to crystalline arsenic. The intensity of these bands decreased almost linearly on etching from one to 14 minutes, indicating the As was dispersed throughout the oxide film.

The proposed reaction

$$As_2O_3 + 2GaAs \rightarrow Ga_2O_3 + 4As \qquad (1)$$
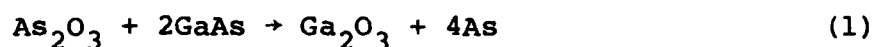
has been discussed by Schwartz (Reference 28) to be the driving force for the appearance of As deposits in the thermally oxidized films. We deposited As_2O_3 on GaAs using a conc. HNO_3 etch. This film was then annealed at 450°C for 60 minutes. Figure 12 shows the Raman data for the two films. The annealed sample gives no indication of As_2O_3 remaining in the film, which is expected because of its sublimation temperature of 200°C. The above reaction should generate four moles of As for every mole of As_2O_3, but the Raman spectrum shows very little intensity from the As bands generated by the 450°C anneal. This particular study

31

indicates that the reaction shown in Equation (1) is not the primary driving mechanism for the appearance of crystalline arsenic in the thermally generated film.

The Auger depth profile data shows arsenic is dispersed throughout the oxide film and is not present as a discreet elemental arsenic layer.

SECTION VII
REMARKS

The Raman scattering experiments were performed with a focused laser beam of 200 μm diameter. With the power of the beam set at 200 mW we can probe surfaces in a nondestructive way. Using 4880Å light, and with the high complex refractive index of GaAs, we are able to look at the near surface (less than 1000Å) of this material.

The thermal oxide film formed in air at 750°C on GaAs is primarily βGa_2O_3. This study indicates there is no reasonable film growth between 200° and 400°C. The temperature region 450° to 650°C shows a film growth that is homogeneous initially and then as the temperature is increased shows some deterioration of the homogeneous layer by growing individual oxide areas. The films grown below 650°C are amorphous and are composed mainly of Ga_2O_3 and crystalline As. Our work indicates metallic arsenic domains are dispersed throughout the initial Ga_2O_3 layer and does not reside as a discreet layer at the interface. These arsenic domains could easily lead to leaky MOS devices.

REFERENCES

1. J. H. Parker, Jr., D. W. Feldman, and M. Ashkin, Phys. Rev. 155, 712 (1967).

2. A. Pincznk and E. Burstein, Phys. Rev. Lett. 21, 1073 (1968).

3. S. Ushioda, Phys. Lett. 33A, 159 (1970).

4. J. P. Russell, Appl. Phys. Lett. 6, 223 (1965).

5. W. G. Fateley, F. R. Dollish, N. T. McDevitt, and F. F. Bentley, "Infrared and Raman Selection Rules for Molecules and Lattice Vibrations: The Correlation Method," Wiley, NY (1972).

6. L. Bragg, G. C. Caringbull, and W. Taylor, "Crystal Structures of Minerals," Cornell University Press (1965).

7. International Tables for X-Ray Crystallography, Vol. 1, N. Henry and K. Lonsdale, Eds., Kynoch, Eng. 2nd Ed. (1965).

8. H. Minden, J. Electrochem. Soc. 109, 733 (1962).

9. M. Rubenstein, J. Electrochem Soc., 113, 540 (1966).

10. B. Sealy and P. Hemment, Thin Solid Films, 22, 539 (1974).

11. B. Schwartz, CRC Crit. Rev. Solid State Sci. 5(4), 609 (1975).

12. D. Butcher and B. Sealy, J. Phys. D: Appl. Phys. 11, 1451 (1978).

13. S. Murarka, Appl. Phys. Lett. 26, 180 (1975).

14. C. Bayliss and D. Kirk, J. Phys. D: Appl. Phys. 9, 233 (1976).

15. I. Shiota, N. Miyamoto, and J. Nishizawa, J. Electrochem. Soc. 124, 1405 (1977).

16. C. Wilmsen and R. Kee, J. Vac. Sci. Technol. 15(4), 1513, (1978).

17. C. Bull and B. Sealy, Phil. Mag. A 37, 489 (1978).

18. H. Takagi, G. Kano, and I. Teramoto, Surf. Sci. 86, 264 (1979).

19. C. Wilmsen, R. Kee, and K. Geib, J. Vac. Sci. Technol. 16(5), 1434 (1979).

20. K. Watanabe, M. Hashiba, Y. Hirobata, M. Nishino, and T. Yamashina, Thin Solid Films 56, 63 (1979).

21. K. Naviatil, O. Ohlidal, and F. Lukes, Thin Solid Films 56, 163 (1979).

22. C. Thurmond, G. Schwartz, G. Kammlot, and B. Schwartz, J. Electrochem. Soc. 127, 1366 (1980).

23. C. Wilmsen, J. Vac. Sci. Technol. 19(3), 279 (1981).

24. K. Frese and S. Morrison, Appl. Surf. Sci. 8, 266 (1981).

25. R. Kee, J. Electrochem. Soc. 125, 998 (1978).

26. G. Abstreiter, E. Bauser, A. Fisher, and K. Ploog, Appl. Phys. 16, 345 (1978).

27. G. Schwartz, J. Griffiths, D. DiStefano, G. Gualtieri, and B. Schwartz, Appl. Phys. Lett. 34, 742 (1979).

28. G. Schwartz, G. Gualtieri, J. Griffiths, C. Thurmond, and B. Schwartz, J. Electrochem. Soc. 127, 2483 (1980).

29. G. Schwartz, B. Schwartz, and J. Griffiths, J. Electrochem. Soc. 127, 2269 (1980).

30. G. Schwartz, SPIE Vol. 276, Optical Characterization Techniques for Semiconductor Technology (1981).

31. T. Nakamura, A. Ushirokawa, and T. Katoda, Appl. Phys. Lett. 38, 13 (1981).

32. H. Stolz, J. Vac. Sci. Technol. 19, 380 (1981).

33. R. Tsu, SPIE Vol. 276, Optical Characterization Techniques for Semiconductor Technology (1981).

34. D. Stirland and B. Straughan, Thin Solid Films 31, 139 (1976).

35. J. Cape, W. Tennant, and L. Hale, J. Vac. Sci. Technol. 14 921 (1977).

36. R. Farrow, R. Chang, and S. Mroczkowski, Appl. Phys. Lett. 31, 768 (1977).

37. R. Zitter, Physics of Semimetals and Narrow-Gap Semiconductors, page 285, Pergamon Press (1970).

38. J. S. Solomon, Appl. Spectros. 30, 46 (1976).

END

FILMED

1-85

DTIC